Remote Sensing of Environment xxx (2014) xxx–xxx

Contents lists available at ScienceDirect

Remote Sensing of Environment

journal homepage: www.elsevier.com/locate/rse

Detecting change in urban areas at continental scales with MODIS data

C.M. Mertes [a,b,*], A. Schneider [a,b], D. Sulla-Menashe [c], A.J. Tatem [d,e], B. Tan [f]

[a] Center for Sustainability and the Global Environment, Nelson Institute for Environmental Studies, Madison, WI, USA
[b] Department of Geography, University of Wisconsin–Madison, Madison, WI 53726, USA
[c] Department of Earth and Environment, Boston University, 685 Massachusetts Avenue, Boston, MA 02215, USA
[d] Department of Geography and Environment, University of Southampton, Highfield, Southampton SO17 1BJ, UK
[e] Fogarty International Center, National Institutes of Health, Bethesda, MD 20892, USA
[f] NASA Goddard Space Flight Center, Greenbelt, MD 20771, USA

ARTICLE INFO

Article history:
Received 24 May 2014
Received in revised form 29 August 2014
Accepted 8 September 2014
Available online xxxx

Keywords:
Urban areas
Urbanization
Cities
Land cover
Change detection
Classification
Machine learning
Decision trees
Data fusion
Decision fusion

ABSTRACT

Urbanization is one of the most important components of global environmental change, yet most of what we know about urban areas is at the local scale. Remote sensing of urban expansion across large areas provides information on the spatial and temporal patterns of growth that are essential for understanding differences in socioeconomic and political factors that spur different forms of development, as well the social, environmental, and climatic impacts that result. However, mapping urban expansion globally is challenging: urban areas have a small footprint compared to other land cover types, their features are small, they are heterogeneous in both material composition and configuration, and the form and rates of new development are often highly variable across locations. Here we demonstrate a methodology for monitoring urban land expansion at continental to global scales using Moderate Resolution Imaging Spectroradiometer (MODIS) data. The new method focuses on resolving the spectral and temporal ambiguities between urban/non-urban land and stable/changed areas by: (1) spatially constraining the study extent to known locations of urban land; (2) integrating multi-temporal data from multiple satellite data sources to classify c. 2010 urban extent; and (3) mapping newly built areas (2000–2010) within the 2010 urban land extent using a multi-temporal composite change detection approach based on MODIS 250 m annual maximum enhanced vegetation index (EVI). We test the method in 15 countries in East–Southeast Asia experiencing different rates and manifestations of urban expansion. A two-tiered accuracy assessment shows that the approach characterizes urban change across a variety of socioeconomic/political and ecological/climatic conditions with good accuracy (70–91% overall accuracy by country, 69–89% by biome). The 250 m EVI data not only improve the classification results, but are capable of distinguishing between change and no-change areas in urban areas. Over 80% of the error in the change detection can be related to definitional issues or error propagation, rather than algorithm error. As such, these methods hold great potential for routine monitoring of urban change, as well as for providing a consistent and up-to-date dataset on urban extent and expansion for a rapidly evolving region.

1. Introduction

The demographic transformation toward an urban world has pushed urbanization – population growth as well as the expansion of built-up areas – to the forefront of environmental and development agendas. The consequences of urbanization are largely contingent on the size, location, and configuration of development (Weng, 2001; Zhou et al., 2004), with many environmental impacts exacerbated when new growth is expansive and/or fragmented in form (Alberti, 2005). A meta-analysis of urban expansion indicates that local- to regional-scale studies are geographically biased, leaving even many large cities unstudied (Seto, Fragkias, Güneralp, & Reilly, 2011). Detailed maps on regional- to global-scale changes in urban land do not exist. Previous efforts have been sample-based (Angel et al., 2005; Schneider & Woodcock, 2008; Taubenböck, Esch, Felbier, Wiesner, & Roth, 2012), have focused on one country (Homer, Huang, Yang, Wylie, & Coan, 2004; Wang et al., 2012), or have drawn conclusions from datasets with substantial temporal and spatial mismatch or variability in how cities are defined (Seto, Sanchez-Rodriguez, & Fragkias, 2010). Routine monitoring of urban expansion across large areas could therefore provide the spatial information on patterns of urban growth that are essential for understanding differences in socio-economic and political factors that spur different forms of development, as well the social and environmental impacts that result (World Bank, 2014).

Several global maps of c. 2000 urban areas have been produced in the past decade (Bhaduri, Bright, Coleman, & Dobson, 2002; CIESIN,

* Corresponding author.
E-mail address: cmertes@wisc.edu (C.M. Mertes).

http://dx.doi.org/10.1016/j.rse.2014.09.023
0034-4257/

Fig. 1. Maps of the East Asia region illustrating (a) the study area extent defined by known locations of urban land, and (b) Olson's biome designation, used to delineate areas of similar ecoclimatic characteristics for data processing.

Please cite this article as: Mertes, C.M., et al., Detecting change in urban areas at continental scales with MODIS data, *Remote Sensing of Environment* (2014), http://dx.doi.org/10.1016/j.rse.2014.09.023

2004; Elvidge et al., 2007; Schneider, Friedl, Mciver, & Woodcock, 2003) which have demonstrated the value of large-area maps of urban extent/expansion for assessment of arable land (Avellan, Meier, & Mauser, 2012; Tan, Li, Xie, & Lu, 2005), water quality/availability (McDonald et al., 2011), natural resources (Lambin & Meyfroidt, 2011), habitat loss (Radeloff et al., 2005) and biodiversity (Guneralp & Seto, 2013); air pollution monitoring and associated impacts to human health (Grimm et al., 2008); and regional-global modeling of climate (Oleson, Bonan, Feddema, Vertenstein, & Grimmond, 2008), hydrological (McGrane, Tetzlaff, & Soulsby, 2014), and biogeochemical cycles (Nordbo, Jarvi, Haapanala, Wood, & Vesala, 2012; Zhao, Zhu, Zhou, Huang, & Werner, 2013). These maps have also proven vital for investigating socioeconomic issues, including population distribution (Jones & O'Neill, 2013), spatial patterns of disease risk (Tatem, Noor, von Hagen, Di Gregorio, & Hay, 2007; Wilhelmi, de Sherbinin, & Hayden, 2013), poverty (Elvidge et al., 2009), and economic growth (Chen & Nordhaus, 2011), and for planning and policy in developing-country cities that lack this information (Scott et al., 2013).

While remote sensing of land cover change for large areas has become common in many types of landscapes (Hansen et al., 2013; Zhang et al., 2003), mapping urban expansion globally has remained relatively difficult: urban areas are rare, their features are small, they are heterogeneous in both material composition and configuration, and the form, rates, and spectral–temporal signatures of urban expansion are highly variable across locations (Jensen & Cowen, 1999; Kontgis et al., 2014; Maktav, Erbek, & Jürgens, 2005; Potere, Schneider, Schlomo, & Civco, 2009). In addition, cost and data availability generally necessitate the use of coarse (250–1000 m) or moderate (20–30 m) resolution data for continental scale mapping, thereby compounding the issue of land cover 'mixing' due to the large ground resolution cell.

The primary objective of this work was to develop a methodology to monitor urban land expansion at continental to global scales. Building on our past work using Moderate Resolution Imaging Spectroradiometer (MODIS) data to map global urban extent (Schneider, Friedl, & Potere, 2010, Schneider et al., 2003), we developed a methodology to resolve the spectral and temporal ambiguities between urban/non-urban land and stable/changed areas by: (1) spatially constraining the study extent using known locations of urban land; (2) integrating multisource satellite data to classify c. 2010 urban extent; and (3) employing multitemporal composites of MODIS 250 m maximum enhanced vegetation index (EVI) observations in a change detection approach to map newly built areas (2000–2010) within the 2010 urban land extent. This method is built on one critical assumption: any conversion of land to urban uses is unidirectional and absolute, and thus, any urban expansion 2000–2010 (regardless of location near/far from the city) will be urban land in 2010.

We test and implement this methodology for 15 countries in East and Southeast Asia (Fig. 1, hereafter East Asia). In doing so, we set a second objective to generate a new dataset depicting recent urban land expansion across the region (Schneider et al., in press). The rapid economic growth and high rates of urbanization characterizing many areas in the region have resulted in a high demand for timely land information for researchers, land use managers, governing institutions and the private sector. East Asia also provides a sound test case for method validation, as the predominance of cloud cover and complex urban landscapes in the region require methods that are robust to missing/noisy data. In the following sections, we outline the background, describe the methods and results, and finally, conclude with a discussion of lessons learned from this research.

2. Background

To map urban expansion across large areas, we draw on three areas in the remote sensing literature: (a) global monitoring of urban land, (b) change detection methods for urban areas, and (c) change detection over large areas.

2.1. Global mapping of urban areas

Eight different teams have developed global maps that depict the spatial extent of urbanization c. 2000 (Gamba & Herold, 2009), while others have developed proof of concept studies (Taubenböck et al., 2012; Zhang & Seto, 2011). Unfortunately, existing global maps exhibit a great deal of variability in how urban areas are characterized, evident from the areal estimates of urban land that range from 300,000 to 3 mil km^2 (Schneider et al., 2010). The definitional problems are twofold. First, any number of operational definitions of 'urban' are employed, ranging from functional definitions related to human land use (Balk et al., 2004; Zhang & Seto, 2011), administrative boundaries (Deichmann, Balk, & Yetman, 2001), or population size and density (Bhaduri, Bright, Coleman, & Dobson, 2002), to physical definitions based on land cover (Elvidge et al., 2007; Schneider et al., 2003) or

Table 1
Datasets used to define the study extent in East Asia for satellite image processing.

Dataset	Producer	Description	Location	Website or citation
MODIS 500 m map of global urban extent	University of Wisconsin–Madison	Map of 88,578 urban patches >1 km^2 used to verify, geolocate, and update city points.	Global	http://www.sage.wisc.edu
GRUMP city points	Center for International Earth Science Information Network (CIESIN), Columbia University, International Food Policy Research Institute (IFPRI), World Bank, Centro Internacional de Agricultura Tropical (CIAT)	Point dataset of 67,935 cities, towns and settlements.	Global	http://sedac.ciesin.columbia.edu
Urban agglomerations with >750,000 inhabitants, 2011	United Nations Department of Economic and Social Affairs Population Division	Point dataset of 633 cities >750,000 persons.	Global	http://esa.un.org/unup/GIS-Files/gis_1.htm
Universe of cities	Angel, Lincoln Institute of Land Policy	Point dataset of 3943 cities >100,000 persons.	Global	Angel (2012). *Planet of Cities*. Cambridge, Massachusetts, Lincoln Institute of Land Policy.
Chinese city point data	Chinese Academy of Sciences	Point dataset of 664 cities.	China	Chinese Academy of Sciences (2011). Beijing, China.
Google Earth populated places	Google Earth Pro v7.1. Layers: populated places	City point location used to verify, geolocate, and update city points.	Global	http://www.google.com/earth

Abbreviations: Moderate Resolution Imaging Spectroradiometer (MODIS), Global Rural–Urban Mapping Project (GRUMP).

Please cite this article as: Mertes, C.M., et al., Detecting change in urban areas at continental scales with MODIS data, *Remote Sensing of Environment* (2014), http://dx.doi.org/10.1016/j.rse.2014.09.023

Table 2
Remote sensing and training datasets used to map c. 2010 urban extent and 2000–2010 urban expansion. Abbreviations: Moderate Resolution Imaging Spectroradiometer (MODIS), Bidirectional reflectance distribution function (BRDF), System for Terrestrial Ecosystem Parameterization (STEP), Enhanced Vegetation Index (EVI).

	Dataset	Description	Source	Location	Time period	Spatial unit
Classification c. 2010	MCD43A4, MCD43A2	MODIS nadir BRDF-adjusted reflectance (NBAR) and quality product 8-day composites	MODIS Land Team, Boston University	Global	Monthly composites, 2009–2011	500 m pixel
	STEP land cover database	Training exemplar database used with NBAR data	Boston University, University of Wisconsin–Madison	Global	c. 2010	500 m–2 km polygon
	MOD09Q1G EVI	MODIS Enhanced Vegetation Index (EVI) 8-day composites	NASA Goddard Space Flight Center	East Asia	Annual growing season maximum, 2009–2010	250 m pixel
	Urban, non-urban training data	Training set database used with EVI data	University of Wisconsin-Madison	East Asia	c. 2010	250 m pixel
	MOD44W	MODIS land-water mask	United States Geological Survey	East Asia	c. 2010	250 m pixel
Change detection 2000–2010	MOD09Q1G EVI	MODIS Enhanced Vegetation Index (EVI) 8-day composites	NASA Goddard Space Flight Center	East Asia	Annual growing season maximum, 2001–2010	250 m pixel
	Urban and urban expansion training data	Training set database used with EVI data	University of Wisconsin–Madison	East Asia	2000–2010	250 m pixel

anthropogenic light emissions (NGDC, 2007). The second is whether the adopted definition is congruent with how the maps are produced, such that the input datasets (e.g., remote sensing, nighttime lights, census data), classification method, and thematic classes align with how urban areas are defined.

Few of the global urban mapping efforts – including new work by the European Space Agency and Google Earth Engine to map c. 2010 urban land – depict *changes* in urban land over time, however. The exception is the GeoCover Land Cover product for 1990–2000 (MDA Federal, 2004), although these data have limited geographic coverage,

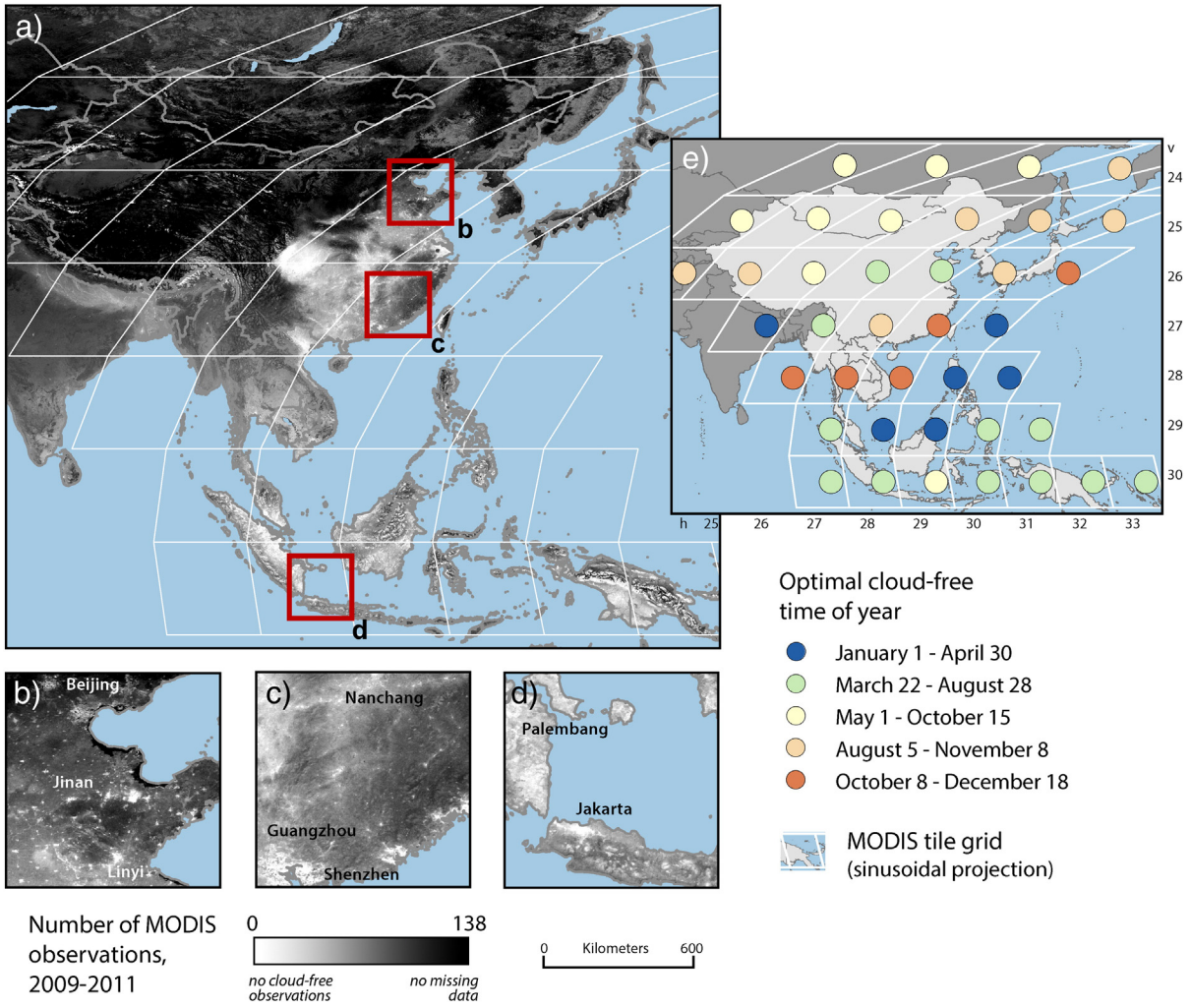

Fig. 2. The distribution of missing data observations in the MODIS 500 m NBAR data for (a) the East Asia study region, and for (b) northeastern China, (c) southeastern China, and (d) central Indonesia. Note the small number of cloud-free observations in cities and tropical/subtropical areas. Panel (e) illustrates the cloud-free time of year for each tile.

Please cite this article as: Mertes, C.M., et al., Detecting change in urban areas at continental scales with MODIS data, *Remote Sensing of Environment* (2014), http://dx.doi.org/10.1016/j.rse.2014.09.023

remain prohibitively expensive, and are becoming outdated for areas witnessing rapid changes since 2000 (Potere et al., 2009). Recent efforts with nighttime lights to monitor urbanization have shown promise, but are limited for mapping urban land expansion explicitly as these data have been found to be a function of demographic, socioeconomic, and land surface variables (Ma, Zhou, Pei, Haynie, & Fan, 2012; Zhang & Seto, 2011).

2.2. Urban change detection

Early approaches to measure urban expansion with remote sensing focused on simple band ratios, image thresholding, and image differencing to discern broad-scale changes at the urban–rural fringe (Howarth & Boasson, 1983; Jensen & Toll, 1982; Martin & Howarth, 1989), while more recent developments accommodate the high spectral variability of urban areas by exploiting spatial or polarimetric dimensions in satellite datasets (Bhaskaran, Paramananda, & Ramnarayan, 2010; Ghimire, Rogan, & Miller, 2010; Shaban & Dikshit, 2001; Taubenböck et al., 2012). Recent studies have also explored data fusion to combine multi-resolution optical data (Deng, Wang, Li, & Deng, 2009), or radar and optical data either during preprocessing (i.e. fusing raw data, Amarsaikhan et al., 2010) or classification (e.g. combining inputs within one algorithm, Corbane, Faure, Baghdadi, Villeneuve, & Petit, 2008; Griffiths, Hostert, Gruebner, & Van der Linden, 2010). As these data fusion techniques use high/very high resolution (VHR) optical data or radar imagery, they have only been applied at the scale of individual cities or neighborhoods (Bhaskaran et al., 2010; Pacifici, Chini, & Emery, 2009; Pesaresi, 2000) where obtaining full coverage is feasible.

2.3. Change detection over large areas

New access to Landsat data has generated a boom in their use for large-area applications (Wulder, Masek, & Cohen, 2012), yet several barriers to their widespread adoption have yet to be resolved. Data availability is still hampered by cloud cover (35% on average, Ju & Roy, 2008), gaps from the scan line corrector failure of Landsat 7 (22% per scene on average, Storey, Scaramuzza, & Schmidt, 2005), and data discontinuities in the archives. While some data issues have been resolved by the unprecedented availability of the Landsat archives, processing these scenes for large areas remains time- and labor-intensive due to the small scene footprint (e.g., East Asia is covered by more than 1500 Landsat footprints). The advantages of coarse resolution data for these applications are therefore clear: comprehensive areal coverage, large image footprints, routine monitoring, archival depth, and perhaps most importantly, frequent data acquisition (global coverage every 1–2 days). Moreover, many methods developed for coarse resolution data will become increasingly viable for Landsat as technical solutions to address data quality and availability continue to be advanced.

3. Definitions

An important first step in the methodology is establishing a clear conceptual framework for defining the urban environment. Representations of urban areas derived from satellite data are most congruent with definitions based on the surface properties that they measure (Potere & Schneider, 2007). Therefore, we define urban areas as locations dominated by constructed surfaces, where dominated implies >50% coverage of a pixel. Spaces that perform an urban function but are not made up of

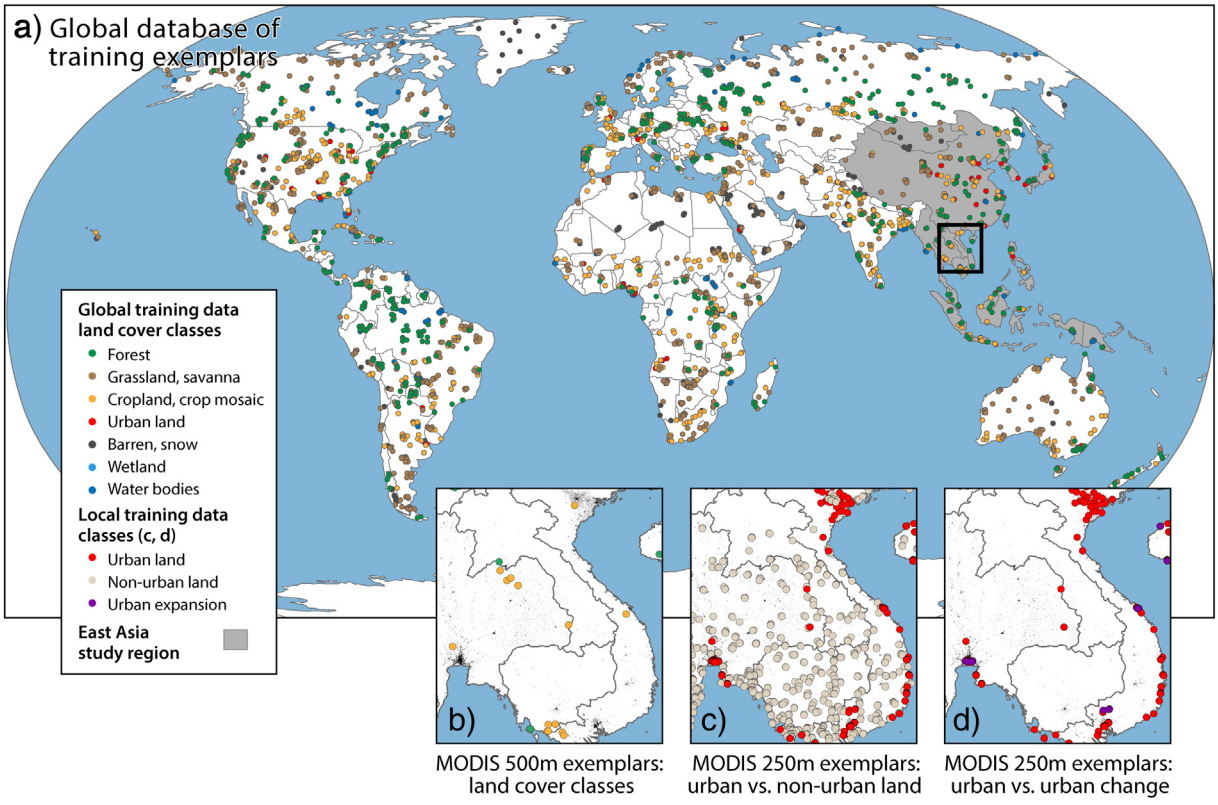

Fig. 3. Global (a) and local views (b–d) of the three training datasets compiled for this research. To classify c. 2010 urban land using the MODIS 500 m data, we rely on a global distribution of >2000 training sites (Friedl et al., 2010) (a, b). This database was updated and augmented with an additional 400+ training sites drawn from a stratified random sample of 250 locations in East and Southeast Asia. To create the a priori urban probability surface using MODIS 250 m data, we collected training data on a tile-by-tile basis for urban and non-urban areas (c). We then adapted (c) to represent stable urban land and urban expansion, 2000–2010 (d), for use in the change detection approach.

Please cite this article as: Mertes, C.M., et al., Detecting change in urban areas at continental scales with MODIS data, *Remote Sensing of Environment* (2014), http://dx.doi.org/10.1016/j.rse.2014.09.023

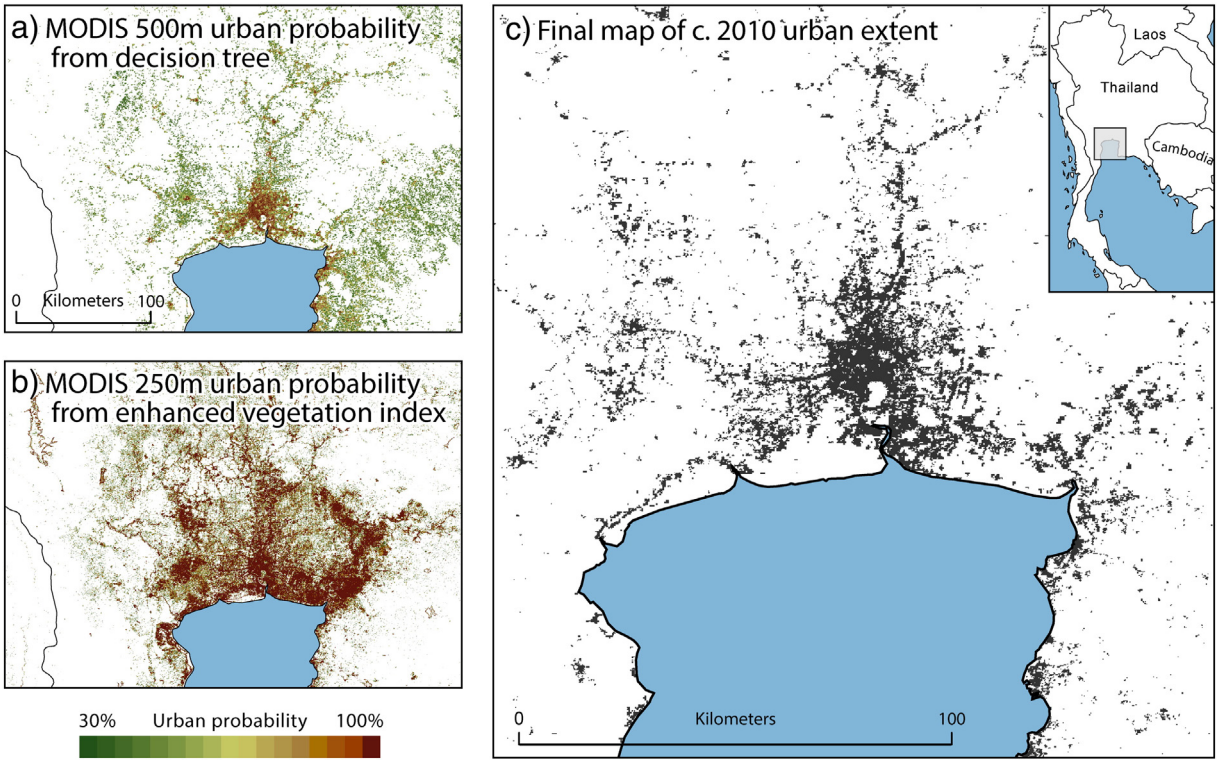

Fig. 4. The data fusion approach used to map c 2010 urban extent for Bangkok, Thailand, illustrating (a) the urban class probability from the MODIS 500 m supervised decision tree classification; (b) the a priori surface for urban land developed from the MODIS 250 m enhanced vegetation index data; and (c) the final map of urban extent from the fusion of the (a) and (b) using Bayes' Rule.

constructed surfaces (e.g. parks, golf courses, green spaces) are not considered urban land. We also define a minimum mapping unit (MMU) of 0.56 km^2 (3 × 3 250 m pixels) as the smallest contiguous area of built-up land reliably represented using 250–500 m MODIS inputs. Conversely, areas within urban areas that do not have built-up surfaces are characterized as non-urban land if they exceed the MMU.

The approach to monitor urban change is based on the premise that any conversion of land to urban cover during the period 2000–2010 will appear as urban land in 2010. The assumption that urban development is irreversible is commonly adopted for land change studies (Carrion-Flores & Irwin, 2004; Schneider, 2012; Seto et al., 2011; Taubenböck et al., 2012) and in practice holds true especially at the temporal scale of interest (e.g. decade). Housing demolition does occur within the study region, but the result is land modification or redevelopment rather than land conversion. In this research, only conversion of non-urban to urban land is considered 'urban expansion,' and all areas converted to built-up surfaces are labeled urban expansion regardless of location within the urban fabric, at the urban fringe, or in peri-urban or rural areas.

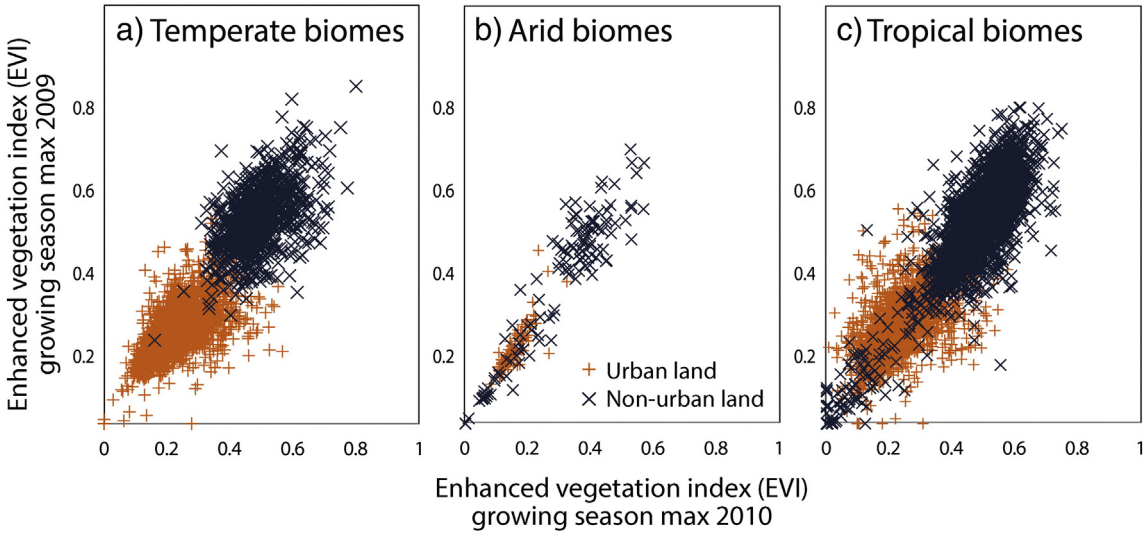

Fig. 5. Maximum enhanced vegetation index (EVI) values for the 2009 and 2010 growing seasons for urban and non-urban exemplars in temperate, arid/semi-arid, and tropical biomes, highlighting the ability of EVI data to discriminate between the two classes. A linear boundary can nearly be fit to the data in temperate zones, and clustering is visible in arid and tropical zones as well, indicating that EVI is informative in these regions as well.

Please cite this article as: Mertes, C.M., et al., Detecting change in urban areas at continental scales with MODIS data, *Remote Sensing of Environment* (2014), http://dx.doi.org/10.1016/j.rse.2014.09.023

Table 3
A comparison of results from the logistic regression models used to estimate an urban/non-urban probability surface with MODIS 250 m enhanced vegetation index (EVI) data. Models were tested with (a) different explanatory variables, and (b) different methods of training data collection.

	Sample size (n)	Number of predictors (x_i)	Number of significant predictors $\alpha = 0.05$ (x_i)	Area under ROC curve
a. Predictor variables				
1 Growing season, all 8-day observations (2010)	1237	23	9	96.0
2 Growing season maximum (2009)	1237	1	1	94.6
3 Growing season maximum (2010)	1237	1	1	93.5
4 Growing season maximum (2009, 2010)	1237	2	2	98.6
5 Growing season maximum (2001, 2009, 2010)	1237	3	2	97.5
b. Method of training data collection (using model 3)				
6 STEP database (Google Earth imagery)	3611	1	1	79.7
7 250 m pixels (MODIS imagery)	1237	1	1	93.5

Abbreviations: Moderate Resolution Imaging Spectroradiometer (MODIS), System for Terrestrial Ecosystem Parameterization (STEP).

4. Data and methods for monitoring urban expansion

4.1. Overview

After defining the study extent, we characterize urban expansion 2000–2010 by: (1) classifying c. 2010 urban land, and (2) locating areas of change within the c. 2010 urban extent.

4.2. Delineating the study area extent

We constrained the East Asia study region to known locations of urban land. To do this, we synthesized all contemporary city point data available (gazetteers, city lists, etc., Table 1) with a c. 2001 map of urban extent developed using an ensemble decision tree classification of the spectral and temporal information in one year of 500 m MODIS observations (Schneider, Friedl, & Potere, 2009). This map has been shown to have the highest locational accuracy of the available maps for the region and a zero omission rate of cities globally (Potere et al., 2009). Circa 2010 point data were then used in all cases possible to ensure all cities >100,000 persons – including those that grew from small settlements to cities >100,000 from 2000 to 2010 – were included in the study extent. In cases where the city points did not align with the 2001 MODIS map of urban areas, city point locations were manually checked against Google Earth data and adjusted as necessary. Contiguous patches of urban land >1 km^2 present in the c. 2001 MODIS map that did not intersect with a city point from any point source were similarly checked in Google Earth, labeled by place name, and included in the dataset if the patch was indeed built-up. Finally, urban patches were categorized into small, medium, and large classes based on their areal extent and population, and then buffered by 5, 25, and 100 km, respectively, to create the final study extent. The study extent represents 30% of the total land area in the region.

Previous work has demonstrated that the controls exerted on land cover and the structure of human settlements by climate, vegetation, and ecosystem characteristics make biome designations useful for stratifying data for continental-scale land cover change (Clark, Aide, & Riner, 2012) and urban applications (Schneider et al., 2009). Using Olson et al.'s (2001) biome classification, the study region was delineated into nine biomes covering temperate, tropical and arid regions (Fig. 1b) used for classification, change detection, and accuracy assessment.

Table 4
Tier one accuracy (urban vs. non-urban land) by country, including user's and producer's accuracies for the urban class.

Country	Tier one accuracy (%)				Test sites (#)	
	Overall	Producer's	User's	Overall, >0.56 km^2 patches only	Total	Urban
Myanmar	93	100	68	93	95	15
North Korea	93	88	64	92	67	8
South Korea	91	71	81	91	215	41
Laos	90	100	60	95	21	4
Cambodia	89	89	89	88	18	9
Thailand	87	73	58	88	324	51
Japan	86	91	74	87	563	185
Philippines	86	94	62	86	227	48
Indonesia	85	84	66	86	529	132
Singapore	85	89	80	85	20	9
Vietnam	85	77	68	86	209	53
China	83	85	62	83	4034	1042
Taiwan	80		0	80	5	0
Malaysia	79	97	60	78	201	63
Region	84	85	64	85	6528	1660

Note: Cells left blank indicate that there were no urban sites drawn in the sample.

4.3. Remote sensing data

We exploit the spectral and temporal information in two separate sources of MODIS data: (1) MODIS 500 m multispectral data, and (2) MODIS 250 m enhanced vegetation index (EVI) data (Table 2). Specifically, we use MODIS 500 m Nadir BRDF-Adjusted Reflectance (NBAR) surface reflectance data (Schaaf et al., 2002) for the seven "land" bands (visible to mid-infrared) for 37 tiles in Asia. NBAR data are normalized to a nadir-viewing angle to reduce noise resulting from varying illumination and viewing geometries (Schaaf et al., 2002), and are produced on a temporally rolling 8-day interval to reduce cloud impacts (Roy, Lewis, Schaaf, Devadiga, & Boschetti, 2006). We rely on EVI rather than the normalized difference vegetation index (NDVI) due to EVI's higher sensitivity to medium- to high-biomass vegetation, which allows EVI to provide better vegetation discrimination in the tropical region of the study area.

In the NBAR data, missing observations frequently occur within/near cities since bright urban surfaces are often mistakenly removed during cloud screening (Leinenkugel, Kuenzer, & Dech, 2013) (Fig. 2). Optimal data were therefore selected for each tile (between 11 and 21 contiguous 8-day observations, Fig. 2e) based on the season with the greatest data availability for urban areas (see S1 for more details). The 8-day NBAR observations were then aggregated to 32-day mean value composites to reduce the temporal correlation and the frequency of missing values from cloud cover. Feature selection was undertaken manually by testing different combinations of inputs, metrics, and compositing periods in several pilot trials based on domain knowledge. The final input features included the monthly (32-day) minima, maxima, means, and variances for each band and vegetation indices, as well as annual metrics calculated using only observations from the cloud-free season for each tile.

At 250 m resolution, we rely solely on EVI data, since vegetation removal has been shown to be an important indicator of urban land conversion (Schneider, 2012; Stefanov, Ramsey, & Christensen, 2001). Because unfiltered MODIS 250 m data are noisy and have a large number of missing observations, we temporally smoothed the data using a modified asymmetric Gaussian filter within an augmented version of TIMESAT (Jönsson & Eklundh, 2002), and then fit a curve to the data that approximates the phenological pattern to fill data gaps (Gao et al.,

Please cite this article as: Mertes, C.M., et al., Detecting change in urban areas at continental scales with MODIS data, *Remote Sensing of Environment* (2014), http://dx.doi.org/10.1016/j.rse.2014.09.023

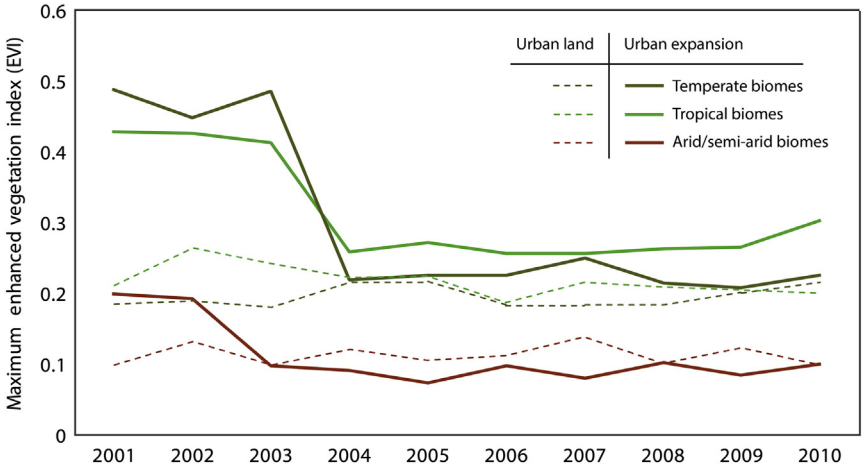

Fig. 6. Enhanced vegetation index (EVI) signatures (growing season maximum for each year 2001–2010, training data mean for each region) depicting differences in trajectories for urban areas and urban expansion in different biomes.

2008; Tan, Morisette, & Wolfe, 2011). The result is a high-quality dataset shown to be suitable for both classification and direct assessment of EVI values (Tan et al., 2011). We selected the MODIS EVI data for the growing season in each tile, defined for all tiles as the 23 observations spanning March through September, and then computed the maximum EVI from these values for each year, 2001–2010.

4.4. Classification of 2010 urban extent

To classify 2010 urban extent, we rely on an ensemble method which uses a supervised decision tree as the base algorithm (C4.5, Quinlan, 1993). Decision trees are capable of accommodating high intra-class variability, and thus have been widely utilized for large area mapping of land cover (Friedl et al., 2002; Hansen, Townshend, Defries, & Carroll, 2005) and urban areas (Schneider et al., 2009). Ten trees are estimated using boosting, a technique that improves class discrimination by iteratively training classifiers based on different weightings of the training data. Because a class label is assigned with each iteration of the boosting algorithm, the ensemble of trees provides a probability estimate for each class at every pixel (McIver & Friedl, 2001). Although the least cloudy season was isolated for each tile (Section 4.2), we used three years of MODIS 500 m data (2009–2011) for the selected season to ensure at least one quality observation for each pixel.

The training data for the 500 m MODIS classification included the System for Terrestrial Ecosystem Parameterization (STEP) database, a set of >2000 exemplars collected from Google Earth and Landsat data for 17 classes (Friedl et al., 2002, 2010). This globally comprehensive database was updated and augmented with >400 sites drawn from a stratified random sample of 250 locations within East Asia (Fig. 3a, b). All sites were collected as 0.5–2.0 km^2 polygons of uniform land cover interpreted using Google Earth imagery.

The results of the MODIS 500 m classification characterized cities well (Fig. 4a), but showed confusion between urban classes and mixed vegetation classes in areas outside cities. To help resolve the spectral ambiguities among these mixed classes, we employed a decision-level data fusion technique using the vegetation information within the 250 m MODIS EVI temporal profiles to refine the classification results (Fig. 4). Methods to monitor vegetation dynamics often employ time-series spectral profiles of vegetation indices (Bradley et al., 2007; Martínez & Gilabert, 2009; Zhang et al., 2003), as the frequent data points provide better discrimination of signal from noise and make it possible to link vegetation phenology to spectral trajectories (Kennedy, Cohen, & Schroeder, 2007). When the retrieval of phenological markers is not relevant, temporal compositing can significantly reduce data volumes and negatively-biased noise from cloud contamination (Fisher, Mustard, & Vadeboncoeur, 2006) while still retaining the temporal characteristics related to land cover (Borak, Lambin, & Strahler, 2000; Clark et al., 2012). Past work has demonstrated that the peak greenness achieved in urban areas is often distinct from nearby land cover types (Schneider et al., 2010). However, this separability varies with climate and biome (Fig. 5). Therefore, we leverage maximum EVI data by biome to calculate probabilities of urban land. Although they are weighted similarly to the probabilities derived from the 500 m MODIS data, we treat these as prior probabilities where the ancillary vegetation information (EVI) provides a local likelihood estimate for membership in both the urban and nonurban classes, thus allowing it to be incorporated into the classification using Bayes' Rule.

To compute the prior probabilities, we defined a logistic regression model using the growing season maxima for the smoothed, gap-filled MODIS EVI data. The model is defined using a binomial distribution and the expression

$$P(U_{LR}) = \frac{e^{V_i}}{1 + e^{V_i}} \quad (1)$$

where $P(U_{LR})$ is the probability that a pixel is urban, and V_i is provided by a multiple linear regression model. Several trials were conducted to model the relationship between EVI and urban areas using different predictor variables (Table 3, models 1–5). Based on the predictive power of the model, given by the area under the receiver operating characteristic (ROC) curve, and the hypothesis test of each variable coefficient (Table 3), the results showed that model 3 outperformed the others. Thus, we model V_i as:

$$V_i = \beta_0 + \beta_1 EVI2009_i + \beta_2 EVI2010_i \quad (2)$$

where $EVI2009_i$ and $EVI2010_i$ are the maximum EVI observations for 2009 and 2010 for the ith pixel, β_1 and β_2 are their coefficients, and β_0 is the intercept. We also found that a model trained with pixels from visual interpretation of the 250 m data outperformed the model trained with the relatively larger 0.5–2 km^2 STEP exemplars selected in Google Earth (Table 3, models 6–7).

We constructed three separate logistic regression models for temperate, tropical and arid regions (the biome groupings are shown in Fig. 1b). Training data were collected for urban and non-urban sites

Please cite this article as: Mertes, C.M., et al., Detecting change in urban areas at continental scales with MODIS data, *Remote Sensing of Environment* (2014), http://dx.doi.org/10.1016/j.rse.2014.09.023

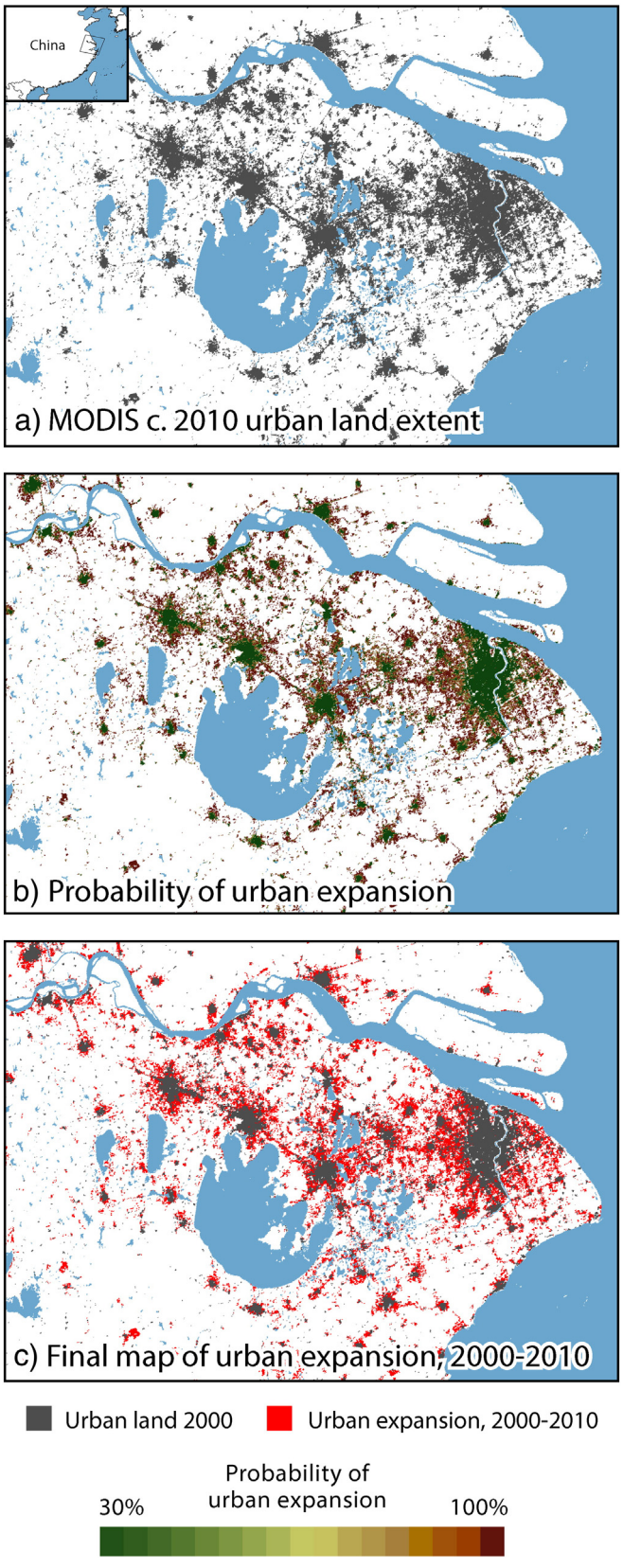

Fig. 7. An illustration of the steps used to characterize urban expansion for the greater Shanghai, China, region: (a) the final map of c. 2010 urban land is used to mask the area of interest; (b) a multi-date composite change detection method is used to generate the probability of urban expansion; and (c) the final map of urban land and urban expansion, after the urban expansion probabilities have been thresholded based on visual interpretation of the probability map (b) in Google Earth.

for each model (Fig. 3c) so greater local representation could be achieved in each region. The regression coefficients were estimated within MATLAB (2011) for each model using an iterative maximum likelihood estimation method for 80% of the training data. The remaining 20% of data were used to assess model performance (Table 4). The Wald test results confirmed that the coefficients for each model were significant at $p < 0.05$ and therefore contributed to the regression (Table S2). The ROC areas were 92, 84, and 76% for temperate, tropical, and arid biomes, respectively, indicating that these models are suitable for predicting the presence of urban areas.

In the last step of the c. 2010 urban classification, we adjusted the prior probabilities from the 250 m MODIS data, $P(U_{LR})$ by the conditional probabilities from the decision trees $P(U_{DT})$. Following Bayes' Rule, we estimate the posterior probabilities $P(Urban)$ as:

$$P(Urban) = \frac{P(U_{DT}) \cdot P(U_{LR})}{\sum_i P(U_{DT}) \cdot P(U_{LR}) + ((1-P(U_{DT})) \cdot (1-P(U_{LR})))}. \quad (3)$$

The posterior probabilities are compared to Google Earth VHR imagery to select an appropriate threshold for defining the urban class. These thresholds were selected at a natural break in the data for each tile or subset of tile (if the tile covers multiple biomes) based on local characteristics and data quality in each area. In temperate biomes, for example, a test of the training data indicated that urban pixels tend to achieve a much higher probability of class membership in the urban class (on average, 94%) than those in arid or tropical regions (on average 51% and 35%, respectively). This occurs because temperate regions have higher quality satellite data, larger amounts of training data, and greater spectral separability between urban and surrounding land cover types than in arid or tropical regions (Fig. 5).

Finally, post-processing refinements were made to finalize the urban extent map. Spurious pixels were removed using a sieve filter, and water bodies were masked using the MODIS 250 m land–water layer (Carroll, Townshend, DiMiceli, Noojipady, & Sohlberg, 2009). As is necessary with many remote sensing-derived maps, a final editing step was conducted by comparing the maps to c. 2010 VHR data in Google Earth and correcting misclassified pixels (note that approximately 10% of all urban areas required some manual editing).

4.5. Mapping change areas (2000–2010)

Capitalizing on the assumption that urban land does not become 'undeveloped', the 2010 urban extent map was used to spatially constrain the change detection process. The change detection method used ten years of growing season maximum EVI data (2001–2010) as input to a boosted decision tree algorithm (C4.5) to classify the c. 2010 urban extent as: (1) built-up in 2000; or (2) urbanized during the 2000-2010 period. The localized training data collected for the logistic regressions (Fig. 3c) were revisited, and all urban sites were labeled as extant urban land, or newly developed urban land, 2000–2010 (Fig. 3d).

This approach relies on the observed relationship between EVI and urban areas established previously: any conversion from agriculture, grassland, forest, etc., to developed land is detectable through changes in vegetation (Fig. 6). As urban spectral trajectories and magnitude of change in vegetation signal accompanying urban expansion varies by the region and between different initial land cover types (Fig. 6), it was necessary to construct decision trees and choose breakpoints to threshold the decision tree urban expansion probabilities by subregion (temperate, tropical, arid) in a similar procedure used for the 2010 urban extent map (Fig. 7). Thresholds were chosen using a procedure similar to the one used for the 2010 urban extent map.

Please cite this article as: Mertes, C.M., et al., Detecting change in urban areas at continental scales with MODIS data, *Remote Sensing of Environment* (2014), http://dx.doi.org/10.1016/j.rse.2014.09.023

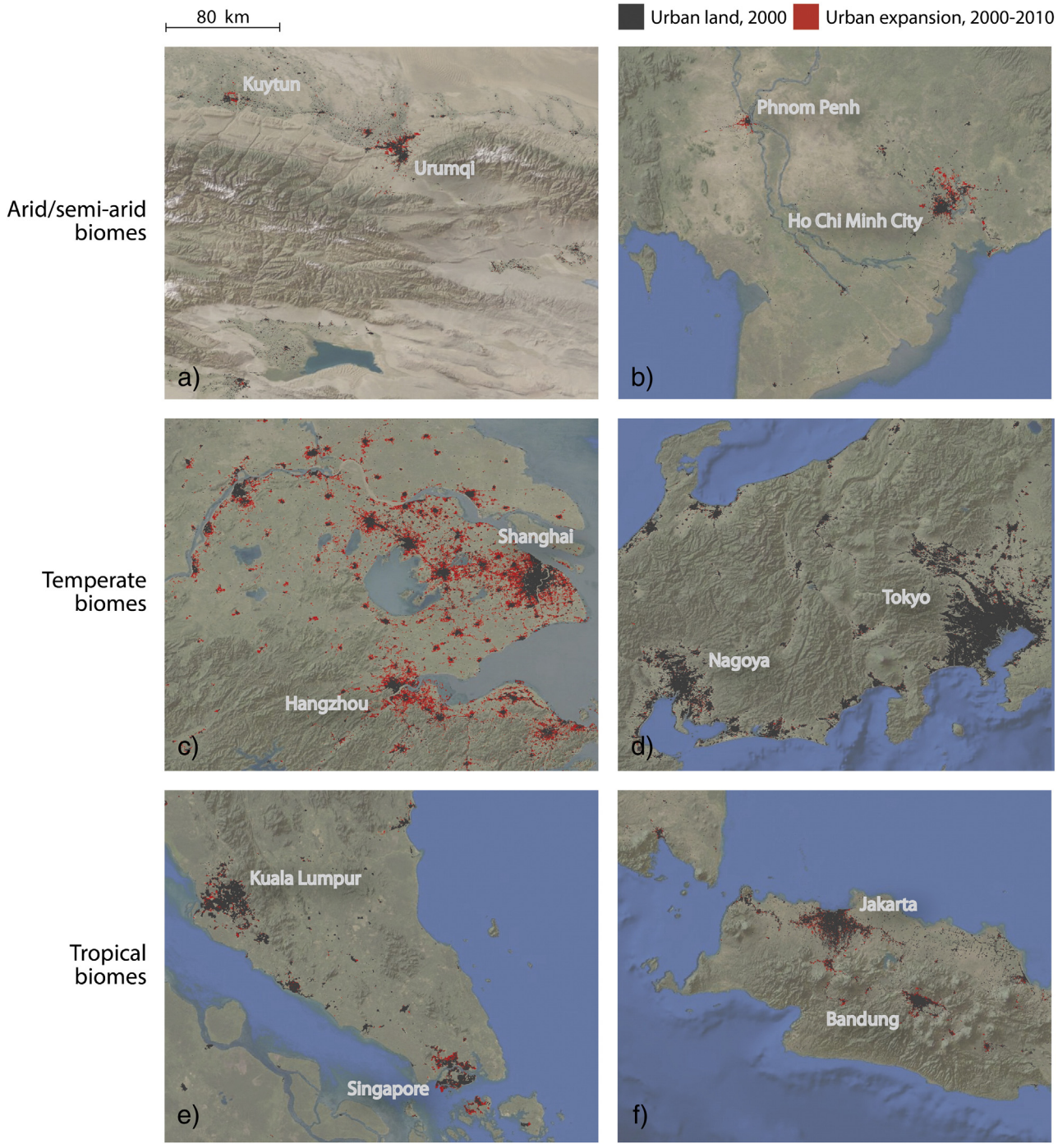

Fig. 8. Urban land and urban expansion 2000–2010 in East Asia for regions spanning several countries and biomes: (a) China — xeric/shrubland; (b) Cambodia and Vietnam — tropical dry forest; (b) (c) China — temperate mixed forest; (d) Japan — temperate mixed forest; (e) Indonesia and Singapore — tropical moist forest; (f) Indonesia — tropical moist forest.

4.6. Accuracy assessment

We examine map accuracy using a two-tiered approach. First, we assess the quality of the 2010 urban classification results, followed by an evaluation of the change detection methodology and urban expansion map accuracy. The tier one test sites were generated using Geodesic Discrete Global Grids (DGGs) (Sahr, White, & Kimerling, 2003), a class of equal-area, uniformly distributed hexagonal partitions of the Earth's surface. To define the sites, we used a DGG with a facet size of 0.132 km^2 and a stratified random sample design drawn from within the study extent. While the final maps were produced at 250 m, this site-based analysis was designed to provide a sampling unit consistent in size with the training data and the 500 m grid of the coarsest resolution MODIS data. The sites were assessed in Google Earth against VHR data ($\leq$4 m) in a double-blind assessment procedure by a team of photo-interpretation analysts, and labeled as urban/non-urban land (tier one), and urban land/urban expansion 2000–2010 (tier two). In all cases, a site had to be >50% of a given land cover type to be labeled as such. A final review of all sites was conducted for quality control and to assign labels in cases where analysts disagreed.

The second tier assessment was designed to quantify the accuracy and efficacy of the change detection methodology, as well as evaluate

Please cite this article as: Mertes, C.M., et al., Detecting change in urban areas at continental scales with MODIS data, *Remote Sensing of Environment* (2014), http://dx.doi.org/10.1016/j.rse.2014.09.023

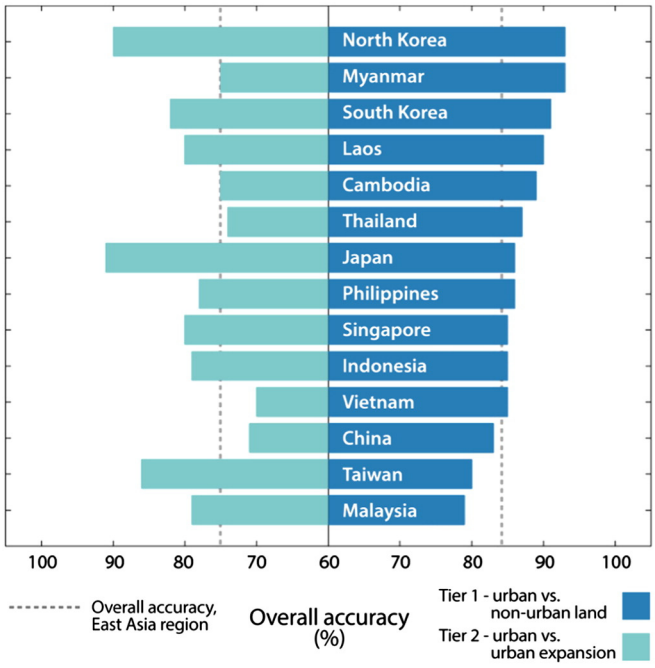

Fig. 9. The overall accuracy results by country for the tier one and tier two assessments.

the accuracy of the urban expansion maps. First, samples were selected in proportion to each country's share of urban land in the region (note that for countries with <1% of urban land, we used a minimum of 20 sites). Second, we sampled across biomes, selecting sites in proportion to the distribution of urban land across the nine biomes (Olson et al., 2001). Once the sample distribution was established (Table S3), we selected sites at random from within a tightly buffered region of the city points using the 250 m MODIS raster grid to ensure that the sample included urban expansion sites. Following the tier one procedure, each site was assessed in Google Earth and assigned one of three labels: urban land, urban expansion, or non-urban land.

5. Results

5.1. Regional and local views

We present the change detection results in Fig. 8 for a subset of metropolitan areas. Visually, these views are in accordance with ground-based evidence and spatial datasets produced at different time points and/or scales. They also indicate that the methods capture new urban development that is contiguous with the urban core across a range of city sizes, as well as patchy growth in peri-urban areas far from the city edge. While the objective of these mapping efforts was to capture all cities >100,000 persons, small cities and villages were also mapped in many areas where the size/composition of the settlements made them spectrally and temporally distinct (e.g., outside Beijing, Fig. 8). The lack of available data on urban expansion at comparable scales limits our ability to cross-examine the map trends, but also underscores an important result: up-to-date, consistent, and spatially-explicit information on the extent and growth of cities is now available for the rapidly evolving region of East-Southeast Asia.

5.2. Tier one accuracy assessment

The overall accuracy of the 2010 map of urban extent (tier one) is 84% (kappa = 0.62), and is fairly consistent across countries (ranging from 79 to 93%, Fig. 9) and biomes (83–100%, Fig. 10). The accuracy was not significantly affected by the inclusion of small patches of urban land (Table 4); overall accuracy drops only 1–2% if these areas are included. Producer's accuracy for the urban class is high for the region (85%), indicating that urban areas are well captured, with few errors of omission (Tables 4, 5). At 64%, the user's accuracy for the region is reasonable, but suggests that map errors are predominantly the result of commission errors where non-urban areas area mislabeled as urban land. As a result, the total urban land area may be overestimated in some locations, particularly Thailand, Malaysia, and Laos, where user's accuracies are <61%.

5.3. Tier two accuracy assessment

The overall accuracy for the urban expansion maps is 75% (kappa = 0.36), slightly lower than the overall c. 2010 accuracy. Similar to the 2010 map, the accuracy measures are representative of urban areas as defined in Section 3.1, with little difference in overall accuracy after small settlements are removed (Table 6). More developed countries (e.g. Japan, Taiwan, South Korea, etc.) generally have higher accuracies (>80%) than other locations likely because of low growth rates in these highly urbanized countries. Overall accuracy rates are higher in temperate and forest biomes than in arid/semi-arid biomes, as are producer's accuracies (9 to 25% above average for forest/temperate, 11 to 21% below average for arid/semi-arid biomes) (Table 7). This result is related to the spectral and temporal signatures of the EVI data used for change detection, since peak EVI in arid regions may be quite similar before and after change (i.e. land outside the city that is spectrally bright and sparsely vegetated is converted to spectrally bright urban land).

5.4. Sources of uncertainty and error in the maps

As expected, the tier two accuracy measures are slightly lower than those for tier one, a result that is to be expected: the errors of the 2010 urban classification propagate through to the urban expansion maps, thus lowering the overall achievable accuracy from the start. To evaluate the methodology and the structure of possible map errors in a more targeted manner, we assessed the source of uncertainty for each misclassified site in the tier two results (n = 513). Each site was reevaluated in Google Earth to determine the likely source of error, and labeled accordingly (Table 8, Fig. 11).

The distribution of errors clearly shows the sensitivity of the tier two assessment to the classification results: 43% of errors are due to classification errors from the initial map of c. 2010 urban land (issue 1, Table 8). While obtaining a perfect classification of 2010 urban land is unrealistic, we can hypothesize that an error-free map of urban land might improve the change detection results. After removing sites mislabeled as non-urban land from the tier two sample, accuracies

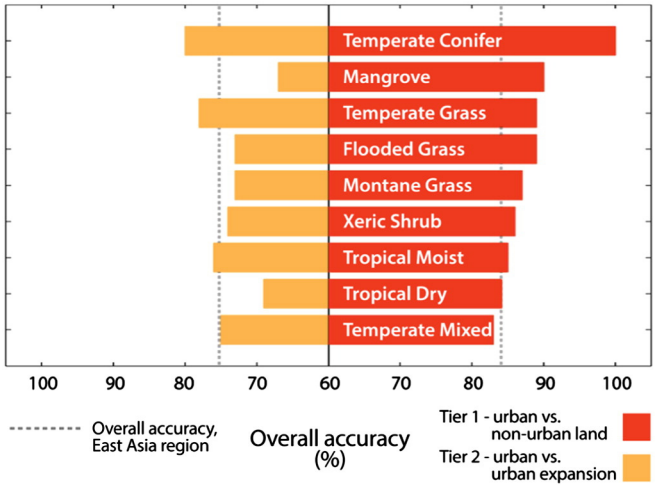

Fig. 10. The overall accuracy results for the tier one and tier two assessments by biome.

Please cite this article as: Mertes, C.M., et al., Detecting change in urban areas at continental scales with MODIS data, *Remote Sensing of Environment* (2014), http://dx.doi.org/10.1016/j.rse.2014.09.023

Table 5
Tier one accuracy (urban vs. non-urban land) by biome, including user's and producer's accuracies for the urban class.

Biome	Tier one accuracy (%)				Test sites (#)	
	Overall	Producer's	User's	Overall, >0.56 km^2 patches only	Total	Urban
Temperate conifer	100	100	100	100	16	2
Tropical conifer	100	100	100	100	6	3
Mangrove	90	91	72	89	97	22
Temperate grass	89	87	70	89	135	30
Flooded grassland	89	92	69	92	53	12
Montane grassland	87	92	57	86	76	13
Xeric shrubland	86	83	74	85	81	24
Tropical moist	85	89	61	85	2390	534
Tropical dry	85	65	67	85	221	54
Temperate mixed	83	84	65	84	3453	965
Region	84	85	64	85	6528	1659

increase 5–15% depending on location, indicating that the change detection method is likely more effective than the overall accuracy results indicate.

Twenty percent of errors appear to be commission error in the urban expansion class, in locations where urban areas are redeveloped or infilled (issue 2, Table 8). As some large cities expand, they consume small villages and built-up areas by clearing old buildings and replacing them with new, spectrally-bright development (Fig. 11d). Likewise, in urbanized areas that are undergoing densification, the spectral response may increase dramatically with new construction. Because our definition of urban land included any built-up areas or settlements, these sites are technically 'urban' in 2000, and remain urban land in 2010. The spectral difference is often large, however, and the change detection approach characterizes these areas as urban expansion accordingly.

An additional 19% of the tier two errors are change detection errors where urban land is mislabeled urban expansion or vice versa, without an obvious indication as to the source of spectral or temporal confusion (issue 3, Fig. 11d). Within this class of errors, the confusion between urban land and urban expansion occurs at a similar frequency, suggesting that there is no bias toward either over- or under-estimating change in the method itself. This error is likely related to the change detection algorithm.

Most of the remaining error (14%) can be traced to the density threshold used to define urban land (issue 4, Table 8). In these cases, the area has some built-up areas c. 2000, but does not meet the >50% threshold to be considered urban land. By 2010, the area fills in, and these areas are then correctly classified as urban land in 2010. A misclassification at the c. 2000 time point leads to a final label of stable urban land when these areas should be labeled urban expansion (Fig. 11b).

Table 6
Tier two accuracy (urban vs. urban expansion) by country, including user's and producer's accuracies for the urban expansion class.

Country	Tier two accuracy (%)				Test sites (#)	
	Overall	Producer's	User's	Overall, >0.56 km^2 patches only	Total	Expansion
Japan	91	100	17	91	243	5
North Korea	90	0		89	20	0
Taiwan	86	71	50	86	28	3
Mongolia	85	0		85	20	0
South Korea	82	71	59	85	40	10
Laos	80	75	86	84	20	7
Singapore	80	75	86	79	20	2
Indonesia	79	36	36	81	148	11
Malaysia	79	8	100	79	67	1
Philippines	78	100	33	78	36	5
Cambodia	75	71	71	75	20	7
Myanmar	75	33	50	79	20	2
Thailand	74	33	20	74	39	5
China	71	64	51	72	1324	166
Vietnam	70	53	80	77	43	15
Region	75	61	50	77	2086	419

Note: Cells left blank indicate that there were no expansion sites drawn in the sample.

6. Discussion and conclusions

Urban expansion remains one of the trickiest and most difficult of land cover types to capture with remote sensing data: both urban land and change areas are rare, and urban spectral classes are neither distinct nor homogeneous, making them difficult to isolate using automated approaches. Therefore, one of the underlying goals of this research was to show how to reduce urban change detection into a manageable problem by restricting the classification areas to those where they will potentially occur. Our methodology leverages information on the location and nature of urban areas and urban expansion using multiple sources of moderate resolution remotely sensed data and several ancillary data sources. We tested the approach for a large and diverse region where urban expansion is often uncoordinated and patchy, and consequently, where urban maps are most challenging to produce, yet most needed. The results reveal several insights for monitoring urban change that are relevant to future studies:

6.1. Data fusion helps yield high map accuracy in complex urban landscapes

While the amounts and quality of remote sensing data are unprecedented, there is still no one 'perfect' data source for the difficult task of mapping urban expansion. We will continue to face limitations in areal coverage and spatial detail, as well as missing data due to cloud cover. Since missing or noisy observations have been shown to significantly impact map accuracy even when advanced data mining algorithms are employed (Rogan et al., 2008; Schneider, 2012), merging data sources and/or products is an important way to overcome these data availability issues.

This work has also shown that combining multiple data sources/products is advantageous given the heterogeneity of urban land and urban growth. Depending on the built-up density, building materials, and amounts/types of vegetative cover, urban areas may resemble other land cover classes more so than they resemble one another (Schneider, 2012; Small, 2006). Our results show that urban areas resemble bare areas in EVI data, while confusion in broadband multispectral data is often between urban areas and other mixed classes. By treating these as complimentary datasets and fusing information derived from both, many errors are offset and higher classification accuracy is achieved.

6.2. Vegetation profiles can reveal urban expansion

Time series data, especially those based on vegetation indices like EVI, have proven fundamental for distinguishing land surface characteristics and monitoring vegetation dynamics in forested or agricultural

Please cite this article as: Mertes, C.M., et al., Detecting change in urban areas at continental scales with MODIS data, *Remote Sensing of Environment* (2014), http://dx.doi.org/10.1016/j.rse.2014.09.023

Table 7
Tier two accuracy (urban vs. urban expansion) by biome, including user's and producer's accuracies for the urban expansion class.

Biome	Tier two accuracy (%)				Test sites (#)	
	Overall	Producer's	User's	Overall, >0.56 km^2 patches only	Total	Expansion
Mangrove	89	72	91	71	18	2
Temperate conifer	80	86	75	80	25	8
Temperate grassland	78	43	33	82	82	9
Tropical moist	76	46	45	77	654	99
Temperate mixed	75	70	51	76	1192	273
Xeric shrubland	74	40	67	78	19	3
Flooded grassland	73	50	100	73	15	1
Montane grassland	73	50	64	75	45	11
Tropical dry	69	73	62	78	36	13
Region	75	61	50	77	2086	419

landscapes (Alcantara et al., 2013; Martínez & Gilabert, 2009; Rahman, Dragoni, Didan, Barreto-Munoz, & Hutabarat, 2013; Zhu, Woodcock, & Olofsson, 2012). The temporal dynamics of EVI are related to variability (e.g. seasonal variation, gradual fluctuation) as well as land cover change (Verbesselt, Hyndman, Newnham, & Culvenor, 2010). We capitalize on both of these frequency components to classify urban land and detect change within urban areas. First, urban areas and other land cover types are often separable if information from multiple seasons is used, since built up lands are predominantly non-vegetated year round while nearby fields or open areas will likely have at least one vegetated season per year. Second, the change information from the longer time series is critical to detect land conversion once urban areas are delineated. Because urban expansion is unidirectional, the use of images from multiple years actually helps confirm whether an area has been developed or whether the drop in the vegetation signal is related to other yearly variability (e.g. crop rotations).

The efficacy and efficiency of EVI temporal information for change detection also highlights the continued utility of MODIS data for urban mapping. Although some urban applications may require greater spatial detail than MODIS provides, the temporal frequency of MODIS is unparalleled, allowing a large number of seasonal and yearly observations that help overcome class confusion due to spectral similarity as well as missing data due to clouds. Indeed, our work provides evidence that it may be possible to pinpoint the timing of change (see Fig. 6). Procedures similar to those used in forest change studies could be adapted for urban environments: given sufficient observations for each year of the study period, a curve-fitting algorithm may be used to isolate a sustained drop in EVI over a moving window of observations (Bradley et al., 2007; Verbesselt et al., 2010). The problem in our study area, however, is that more than half of the region is missing yearly information.

While the multitemporal composite method is highly suited to detect urban change, this analysis also reveals biases that should be considered. First, this method relies on vegetation as an indicator of change, so the technique is limited in some arid regions. Although cities in arid and semi-arid locations are often surrounded by irrigated agriculture, allowing for changes in EVI to be observed, there are locations where bare ground outside the city is converted to built-up land. These changes are difficult to detect using EVI, unless the conversion is accompanied by a sufficient vegetation increase (e.g. street trees, garden plots). For similar reasons, there is an inherent bias toward new, spectrally-bright development; our approach is limited in areas where natural roofing or building materials (e.g. thatched houses) have EVI signals similar to nearby vegetation. In developing our methodology, we were able to overcome both of these biases by tailoring our approach to the biome or location at hand. This allows greater freedom with the method, but also leads to increased user input and greater subjectivity, which may in turn, restrict the utility of the method for some users. However, the range of metrics that can be estimated from time series imagery is vast, and many features have not yet been explored for urban areas (e.g. differences in foliage water content that might be captured by the normalized difference infrared index (NDII), Gao, 1996).

6.3. Ancillary information can help simplify the problem

Urban areas account for just 1–2% of total global land area, and urban expansion within/near these areas occurs infrequently. While the exact patterns and extents of urban areas are not well-known globally, their

Table 8
The potential sources of error in the misclassified test sites of the tier two accuracy assessment.

Issue		Occurrence (%)	Description, examples	Ground truth label 2000 » 2010[a]	Map label 2000 » 2010[a]	No. test sites
1	Classification error	43	Urban commission error where non-urban land is labeled urban land in 2010. Confusion between land without built surfaces (e.g. confusion between urban areas and extraction activities, riparian areas, bare soil, agriculture, etc.) (a) or with low density (<50%) surfaces may occur (b).	Non-urban » Non-urban	Urban » urban	218
2	Redevelopment and/ or increasing built-up density	20	New development occurs in existent urban area, e.g. settlement is cleared and rebuilt (a), or there is an increase in buildings/impervious cover (b), leading to change in spectral brightness. No change in label occurs.	Urban » Urban	Non-urban » urban	105
3	Change detection error	19	Urban land and urban expansion are confused by classifier.	Urban » Urban Non-urban » Urban	Non-urban » urban Urban » urban	57 41
4	Low density urban	14	Area has some built-up areas c. 2000, but does not meet the >50% threshold to be considered urban. Because the area increases to >50% built-up density by 2010, it results in change omission.	Non-urban » Urban	Urban » urban	71
5	Other	5	Other factor was cited, such as uncertainty in photo-interpretation or limited reference imagery.			21

[a] The labels in the table correspond to the class structure as follows: *non-urban land* includes all non-urban → non-urban areas: *stable urban land* includes all urban → urban areas; and *urban expansion 2000–2010* includes non-urban → urban areas.

Please cite this article as: Mertes, C.M., et al., Detecting change in urban areas at continental scales with MODIS data, *Remote Sensing of Environment* (2014), http://dx.doi.org/10.1016/j.rse.2014.09.023

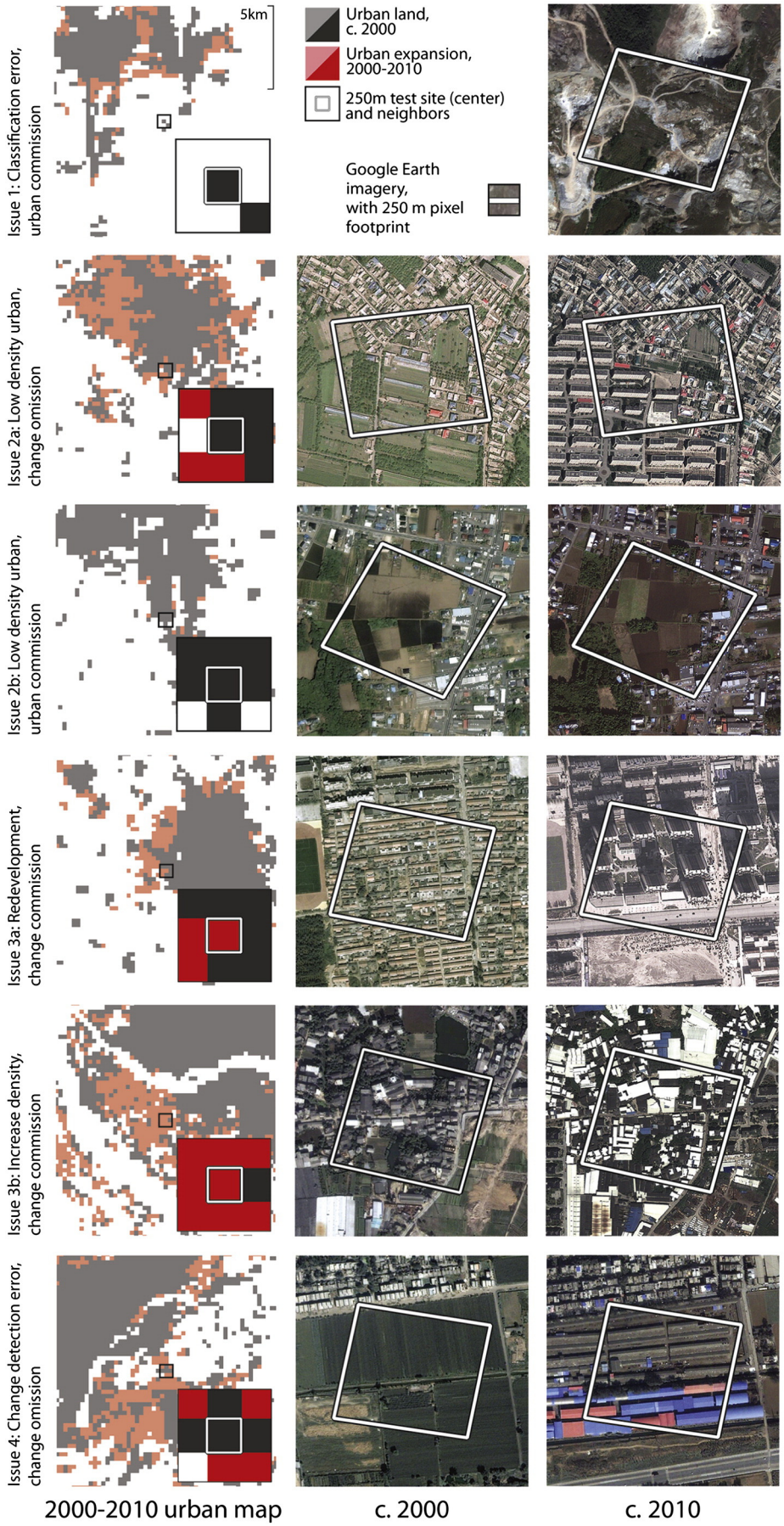

Fig. 11. A sample of the types of issues associated with mislabeled sites in the tier two accuracy assessment of urban land and urban expansion (see x1 for a full description and the frequency of occurrence). The locations of the sites from top to bottom are: Dashiqiao, China; Ibaraki, Japan; Langfang, China; Fuzhou, China; Luoyang, China; Yining City, China.

Please cite this article as: Mertes, C.M., et al., Detecting change in urban areas at continental scales with MODIS data, *Remote Sensing of Environment* (2014), http://dx.doi.org/10.1016/j.rse.2014.09.023

central locations are captured in a variety of public/private databases, including point datasets, city lists, and even online mapping engines. We have shown that the use of very liberal buffers (up to 100 km) applied to a synthesis of these ancillary datasets (Table 1) eliminated 70% of the land extent from the image processing stream. Basing the change detection methodology on the same premise of constraining the area for classification, we were able to work 'backwards' from 2010 to map expansion for the 2000–2010 period. In addition, free, highly-detailed Google Earth imagery was harnessed at nearly every step, from training collection to validation. Our approach allowed these data to be exploited without using them explicitly during image processing, thereby limiting the propagation of errors into the final results and extending the capabilities of free data.

6.4. Steps toward routine monitoring

The demand for maps that depict rates, patterns, and amounts of urban land expansion at regional and continental scales is high and growing, and as a result, smart, efficient ways to characterize change using new and existing data sources will be necessary. Our results suggest that classification of urban land remains a labor-intensive, location-based exercise, but methods to detect urban change are moving closer to routine monitoring if vegetation trajectories and multiple data sources are exploited. Moreover, the method to map urban expansion shown here is particularly relevant given the new c. 2010 global urban maps (none of which depict change) that will become available in 2014–2015 (see proof-of-concept papers from Esch et al., 2013; Gamba & Lisini, 2013; Pesaresi et al., 2013). These spatially-detailed, highly accurate c. 2010 urban extent maps will help improve the methodology by providing a better, more accurate way to constrain the study extent. The majority of the error in our change detection results was attributable to errors in the c. 2010 map we developed, so improvements in this map means higher change detection accuracy can be achieved.

Finally, the emerging digital landscape is providing vast new data sources on urban processes that could be incorporated into mapping methodologies. Data from location-based social networks (e.g. Foursquare) or geo-located internet/social media posts (e.g. Twitter, Facebook, FlickR) are increasingly being exploited to monitor and map disease outbreaks (Signorini, Segre, & Polgreen, 2011) and natural disasters (Gao, Barbier, & Goolsby, 2011; Yates & Paquette, 2011). While the quality and reliability of crowd-sourced and volunteered geographic information must be considered, these datasets provide opportunities for innovation in using humans as sensors.

In sum, global mapping efforts are important because consistent methodologies and definitions facilitate broad scale and comparative analysis, but a 'one size fits all' approach will not provide the best results everywhere. In covering large and diverse regions, specific datasets will be more informative in some regions and less so in others. Likewise, different subsets of data are regionally appropriate. For this work, we process data by subregions according to their cloud cover seasonality and ecoclimatic characteristics. By accommodating regional differences but maintaining consistent definitions, data sources, and methods, this work has provided an up-to-date dataset suitable for both broad-scale and comparative analysis, as well as a framework that can be extended to map urban expansion globally.

Acknowledgments

The authors wish to thank Phil Townsend, Mutlu Ozdogan, Caitlin Kontgis, and two anonymous reviewers for comments on an earlier draft of this manuscript. The authors are grateful to Sarah Graves, Jo Horton, James Rollo, and Ian Schelly for technical support, assistance in data collection, and cartographic expertise. This work was funded in part by support from the World Bank. The funders had no role in study design, data collection and analysis, decision to publish, or preparation of the manuscript.

Appendix A. Supplementary data

Supplementary data to this article can be found online at http://dx.doi.org/10.1016/j.rse.2014.09.023.

References

Alberti, M. (2005). The effects of urban patterns on ecosystem function. *International Regional Science Review, 28*, 168–192.

Alcantara, C., Kuemmerle, T., Baumann, M., Bragina, E. V., Griffiths, P., Hostert, P., et al. (2013). Mapping the extent of abandoned farmland in Central and Eastern Europe using MODIS time series satellite data. *Environmental Research Letters, 8*(3), 035035.

Amarsaikhan, D., Blotevogel, H. H., van Genderen, J. L., Ganzorig, M., Gantuya, R., & Nergui, B. (2010). Fusing high-resolution SAR and optical imagery for improved urban land cover study and classification. *International Journal of Image and Data Fusion, 1*(1), 83–97.

Angel, S., Sheppard, S. C., Civco, D. L., Buckley, R., Chabaeva, A., Gitlin, L., et al. (2005). The dynamics of global urban expansion. *Transport and Urban Development Department Report*. Washington DC: World Bank Publications.

Angel, S. (2012). *Planet of Cities*. Cambridge, Massachusetts: Lincoln Institute of Land Policy.

Avellan, T., Meier, J., & Mauser, W. (2012). Are urban areas endangering the availability of rainfed crop suitable land? *IEEE Geoscience and Remote Sensing Letters, 3*(7), 631–638.

Balk, D., Pozzi, F., Yetman, G., Deichmann, U., Nelson, A., & Bank, T. W. (2004). *The distribution of people and the dimension of place: Methodologies to improve the global estimation of urban extents*. Washington DC: Center for International Earth Science Information Network.

Bhaduri, B., Bright, E., Coleman, P., & Dobson, J. (2002). LandScan: Locating people is what matters. *Geoinformatics, 5*, 34–37.

Bhaskaran, S., Paramananda, S., & Ramnarayan, M. (2010). Per-pixel and object-oriented classification methods for mapping urban features using Ikonos satellite data. *Applied Geography, 30*(4), 650–665.

Borak, J. S., Lambin, E. F., & Strahler, A. H. (2000). The use of temporal metrics for land cover change detection at coarse spatial scales. *International Journal of Remote Sensing, 21*(6–7), 1415–1432.

Bradley, B. A., Jacob, R. W., Hermance, J. F., & Mustard, J. F. (2007). A curve fitting procedure to derive inter-annual phenologies from time series of noisy satellite NDVI data. *Remote Sensing of Environment, 106*, 137–145.

Carrion-Flores, C., & Irwin, E. (2004). Determinants of residential land-use conversion and sprawl at the rural–urban fringe. *American Journal of Agricultural Economics, 86*, 889–904.

Carroll, M., Townshend, J., DiMiceli, C., Noojipady, P., & Sohlberg, R. (2009). A new global raster water mask at 250 meter resolution. *International Journal of Digital Earth, 2*(4), 291–308.

Center for International Earth Science Information Network (CIESIN) (2004). *Global Rural–Urban Mapping Project (GRUMP)*. Alpha Version: Urban Extents (available online at: http://sedac.ciesin.columbia.edu/gpw).

Chen, X., & Nordhaus, W. D. (2011). Using luminosity data as a proxy for economic statistics. *Proceedings of the National Academy of Sciences of the United States of America, 108*, 8589–8594.

Clark, M. L., Aide, T. M., & Riner, G. (2012). Land change for all municipalities in Latin America and the Caribbean assessed from 250-m MODIS imagery (2001–2010). *Remote Sensing of Environment, 126*, 84–103.

Corbane, C., Faure, J. F., Baghdadi, N., Villeneuve, N., & Petit, M. (2008). Rapid urban mapping using SAR/optical imagery synergy. *Sensors, 8*(11), 7125–7143.

Deichmann, U., Balk, D., & Yetman, G. (2001). *Transforming population data for interdisciplinary usages: From census to grid*. Washington DC: Center for International Earth Science Information Network.

Deng, J. S., Wang, K., Li, J., & Deng, Y. H. (2009). Urban land use change detection using multisensor satellite images. *Pedosphere, 19*(1), 96–103.

Elvidge, C. D., Sutton, P., Ghosh, T., Tuttle, B., Baugh, K., Bhaduri, B., et al. (2009). A global poverty map derived from satellite data. *Computers & Geosciences, 35*, 1652–1660.

Elvidge, C., Tuttle, B. T., Sutton, P. C., Baugh, K. E., Howard, A. T., Milesi, C., et al. (2007). Global distribution and density of constructed impervious surfaces. *Sensors, 7*, 1962–1979.

Esch, T., Marconcini, M., Felbier, A., Roth, A., Heldens, W., Huber, M., et al. (2013). Urban footprint processor — Fully automated processing change generating settlement masks from global data of the TanDEM-X mission. *IEEE Geoscience and Remote Sensing Letters, 10*, 1617–1621.

Fisher, J., Mustard, J., & Vadeboncoeur, M. (2006). Green leaf phenology at Landsat resolution: Scaling from the field to the satellite. *Remote Sensing of Environment, 100*(2), 265–279.

Friedl, M. A., McIver, D. K., Hodges, J., Zhang, X., Muchoney, D., Strahler, A., et al. (2002). Global land cover mapping from MODIS: Algorithms and early results. *Remote Sensing of Environment, 83*, 287–302.

Friedl, M. A., Sulla-Menashe, D., Tan, B., Schneider, A., Ramankutty, N., Sibley, A., et al. (2010). MODIS Collection 5 global land cover: Algorithm refinements and characterization of new datasets. *Remote Sensing of Environment, 114*, 168–182.

Gamba, P., & Herold, M. (Eds.). (2009). *Global mapping of human settlements: Experiences, datasets, and prospects*. Boca Raton, Florida: CRC Press.

Gamba, P., & Lisini, G. (2013). Fast and efficient urban extent extraction using ASAR wide swath mode data. *IEEE Journal of Selected Topics in Applied Earth Observations and Remote Sensing, 6*, 2184–2195.

Please cite this article as: Mertes, C.M., et al., Detecting change in urban areas at continental scales with MODIS data, *Remote Sensing of Environment* (2014), http://dx.doi.org/10.1016/j.rse.2014.09.023

Gao, B. C. (1996). NDWI: A normalized difference water index for remote sensing of vegetation liquid water from space. *Remote Sensing of Environment*, *58*, 257–266.

Gao, H., Barbier, G., & Goolsby, R. (2011). Harnessing the crowdsourcing power of social media for disaster relief. *IEEE Intelligent Systems*, *26*(3), 10–14.

Gao, F., Morisette, J. T., Wolfe, R. E., Ederer, G., Pedelty, J., Masuoka, E., et al. (2008). An algorithm to produce temporally and spatially continuous MODIS-LAI time series. *IEEE Transactions on Geoscience and Remote Sensing*, *5*, 60–64.

Ghimire, B., Rogan, J., & Miller, J. (2010). Contextual land-cover classification: Incorporating spatial dependence in land-cover classification models using random forests and the Getis statistic. *IEEE Geoscience and Remote Sensing Letters*, *1*(1), 45–54.

Griffiths, P., Hostert, P., Gruebner, O., & Van der Linden, S. (2010). Mapping megacity growth with multi-sensor data. *Remote Sensing of Environment*, *114*, 426–439.

Grimm, N. B., Foster, D., Groffman, P., Grove, J. M., Hopkinson, C. S., Nadelhoffer, K. J., et al. (2008). The changing landscape: Ecosystem responses to urbanization and pollution across climatic and societal gradients. *Frontiers in Ecology and the Environment*, *6*, 264–272.

Guneralp, B., & Seto, K. C. (2013). Futures of global urban expansion: Uncertainties and implications for biodiversity conservation. *Environmental Research Letters*, *8*(1), 014025 (article).

Hansen, M. C., Potapov, P. V., Moore, R., Hancher, M., Turubanova, A., Tyukavina, A., et al. (2013). High-resolution global maps of 21st century forest cover change. *Science*, *342*, 850–853.

Hansen, M. C., Townshend, J. R. G., Defries, R. S., & Carroll, M. (2005). Estimation of tree cover using MODIS data at global, continental and regional/local scales. *International Journal of Remote Sensing*, *26*, 4359–4380.

Homer, C., Huang, C., Yang, L., Wylie, B., & Coan, M. (2004). Development of a 2001 national land-cover database for the United States. *Photogrammetric Engineering and Remote Sensing*, *70*, 829–840.

Howarth, P. J., & Boasson, E. (1983). Landsat digital enhancements for change detection in urban environments. *Remote Sensing of Environment*, *13*, 149–160.

Jensen, J. R., & Cowen, D. C. (1999). Remote sensing of urban/suburban infrastructure and socioeconomic attributes. *Photogrammetric Engineering and Remote Sensing*, *65*, 611–622.

Jensen, J. R., & Toll, D. L. (1982). Detecting residential land use development at the urban fringe. *Photogrammetric Engineering and Remote Sensing*, *48*, 629–643.

Jones, B., & O'Neill, B. C. (2013). Historically grounded spatial population projections for the continental United States. *Environmental Research Letters*, *8*(4), 044021 (article).

Jönsson, P., & Eklundh, L. (2002). Seasonality extraction by function fitting to time-series of satellite sensor data. *IEEE Transactions on Geoscience and Remote Sensing*, *40*(8), 1824–1832.

Ju, J., & Roy, D. P. (2008). The availability of cloud-free Landsat ETM + data over the conterminous United States and globally. *Remote Sensing of Environment*, *112*, 1196–1211.

Kennedy, R. E., Cohen, W. B., & Schroeder, T. A. (2007). Trajectory-based change detection for automated characterization of forest disturbance dynamics. *Remote Sensing of Environment*, *110*, 370–386.

Kontgis, C. P., Schneider, A., Fox, J., Saksena, S., Spencer, J., & Castrence, M. (2014). Monitoring peri-urbanization in the greater Ho Chi Minh City metropolitan area. *Journal of Applied Geography*, *53*, 377–388.

Lambin, E. F., & Meyfroidt, P. (2011). Global land use change, economic globalization, and the looming land scarcity. *Proceedings of the National Academy of Sciences of the United States of America*, *108*, 3465–3472.

Leinenkugel, P., Kuenzer, C., & Dech, S. (2013). Comparison and enhancement of MODIS cloud mask products for Southeast Asia. *International Journal of Remote Sensing*, *34*(8), 2730–2748.

Ma, T., Zhou, C., Pei, T., Haynie, S., & Fan, J. (2012). Quantitative estimation of urbanization dynamics using time series of DMSP/OLS nighttime light data: A comparative case study from China's cities. *Remote Sensing of Environment*, *124*, 99–107.

Maktav, D., Erbek, F. S., & Jürgens, C. (2005). Remote sensing of urban areas. *International Journal of Remote Sensing*, *26*(4), 655–659.

Martin, L., & Howarth, P. (1989). Change-detection accuracy assessment using SPOT multispectral imagery of the rural-urban fringe. *Remote Sensing of Environment*, *30*(1), 55–66.

Martínez, B., & Gilabert, M. A. (2009). Vegetation dynamics from NDVI time series analysis using the wavelet transform. *Remote Sensing of Environment*, *113*(9), 1823–1842.

MATLAB (2011). *Statistics toolbox release.* Natick, Massachusetts, United States: The MathWorks, Inc.

McDonald, R. I., Green, P., Balk, D., Fekete, B. M., Revenga, C., Todd, M., et al. (2011). Urban growth, climate change, and freshwater availability. *Proceedings of the National Academy of Sciences of the United States of America*, *108*(15), 6312–6317.

McGrane, S. J., Tetzlaff, D., & Soulsby, C. (2014). Influence of lowland aquifers and anthropogenic impacts on the isotope hydrology of contrasting mesoscale catchments. *Hydrological Processes*, *28*(3), 793–808.

McIver, D. K., & Friedl, M. A. (2001). Estimating pixel-scale land cover classification confidence using non-parametric machine learning methods. *IEEE Transactions on Geoscience and Remote Sensing*, *39*, 1959–1968.

MDA Federal (2004). *Landsat GeoCover maps.* (Washington, DC (available online at: http://www.mdafederal.com/geocover/geocoverlc/)).

National Geophysical Data Center (NGDC) (2007). Nighttime lights data. (available online at: http://ngdc.noaa.gov/eog/dmsp.html).

Nordbo, A., Jarvi, L., Haapanala, S., Wood, C. R., & Vesala, T. (2012). Fraction of natural area as main predictor of net CO_2 emissions from cities. *Geophysical Research Letters*, *39*, L20802.

Oleson, K. W., Bonan, G. B., Feddema, J., Vertenstein, M., & Grimmond, C. S. B. (2008). An urban parameterization for a global climate model: 1. Formulation and evaluation for two cities. *Journal of Applied Meteorology and Climatology*, *47*, 1038–1060.

Olson, D. M., Dinerstein, E., Wikramanayake, E., Burgess, N., Powell, G., Underwood, E., et al. (2001). Terrestrial ecoregions of the world: A new map of life on Earth. *BioScience*, *51*, 933–938.

Pacifici, F., Chini, M., & Emery, W. J. (2009). A neural network approach using multi-scale textural metrics from very high-resolution panchromatic imagery for urban land-use classification. *Remote Sensing of Environment*, *113*(6), 1276–1292.

Pesaresi, M. (2000). Texture analysis for urban pattern recognition using fine-resolution panchromatic satellite imagery. *Geographical and Environmental Modelling*, *4*(1), 43–63.

Pesaresi, M., Huadong, G., Blaes, X., Ehrlich, D., Ferri, S., Gueguen, L., et al. (2013). A global human settlement layer from optical HR/VHR RS data: concept and first results. *IEEE Journal of Selected Topics in Applied Earth Observations and Remote Sensing*, *6*, 2102–2131.

Potere, D., & Schneider, A. (2007). A critical look at representations of urban areas in global maps. *GeoJournal*, *69*, 55–80.

Potere, D., Schneider, A., Schlomo, A., & Civco, D. A. (2009). Mapping urban areas on a global scale: Which of the eight maps now available is more accurate? *International Journal of Remote Sensing*, *30*, 6531–6558.

Quinlan, J. R. (1993). *C4.5: Programs for machine learning.* New York: Morgan Kaufmann Publishers.

Radeloff, V. C., Hammer, R. B., Stewart, S. I., Fried, J. S., Holcomb, S. S., & McKeefry, J. F. (2005). The wildland–urban interface in the United States. *Ecological Applications*, *15*(3), 799–805.

Rahman, A. F., Dragoni, D., Didan, K., Barreto-Munoz, A., & Hutabarat, J. (2013). Detecting large scale conversion of mangroves to aquaculture with change point and mixed-pixel analyses of high-fidelity MODIS data. *Remote Sensing of Environment*, *130*, 96–107.

Rogan, J., Franklin, J., Stow, D., Miller, J., Woodcock, C., & Roberts, D. (2008). Mapping land-cover modifications over large areas: A comparison of machine learning algorithms. *Remote Sensing of Environment*, *112*(5), 2272–2283.

Roy, D. P., Lewis, P., Schaaf, C. B., Devadiga, S., & Boschetti, L. (2006). The global impact of clouds on the production of MODIS bidirectional reflectance model-based composites for terrestrial monitoring. *IEEE Transactions on Geoscience and Remote Sensing*, *3*, 452–456.

Sahr, K., White, D., & Kimerling, A. J. (2003). Geodesic discrete global grid systems. *Cartography and Geographic Information Science*, *30*(2), 121–134.

Schaaf, C. B., Gao, F., Strahler, A. H., Lucht, W., Li, X., Tsang, T., et al. (2002). First operational BRDF, albedo nadir reflectance products from MODIS. *Remote Sensing of Environment*, *83*, 135–148.

Schneider, A. (2012). Monitoring land cover change in urban and peri-urban areas using dense time stacks of Landsat satellite data and a data mining approach. *Remote Sensing of Environment*, *124*, 689–704.

Schneider, A., Friedl, M. A., Mciver, D. K., & Woodcock, C. E. (2003). Mapping urban areas by fusing multiple sources of coarse resolution remotely sensed data. *Photogrammetric Engineering and Remote Sensing*, *69*, 1377–1386.

Schneider, A., Friedl, M. A., & Potere, D. (2009). A new map of global urban extent from MODIS satellite data. *Environmental Research Letters*, 044003 (article).

Schneider, A., Friedl, M. A., & Potere, D. (2010). Mapping urban areas globally using MODIS 500 m data: New methods and datasets based on urban ecoregions. *Remote Sensing of Environment*, *114*, 1733–1746.

Schneider, A., & Woodcock, C. E. (2008). Compact, dispersed, fragmented, extensive? A comparison of urban expansion in twenty-five global cities using remotely sensed data, pattern metrics and census information. *Urban Studies*, *45*, 659–692.

Scott, A. J., Carter, C., Reed, M. R., Larkham, P., Adams, D., Morton, N., et al. (2013). Disintegrated development at the rural-urban fringe: Re-connecting spatial planning theory and practice. *Progress in Planning*, *83*, 1–52.

Seto, K. C., Fragkias, M., Güneralp, B., & Reilly, M. K. (2011). A meta-analysis of global urban land expansion. *PLoS One*, *6*, e23777.

Seto, K. C., Sanchez-Rodriguez, R., & Fragkias, M. (2010). The new geography of contemporary urbanization and the environment. *Annual Review of Environment and Resources*, *35*, 167–194.

Shaban, M. A., & Dikshit, O. (2001). Improvement of classification in urban areas by the use of textural features: the case study of Lucknow city, Uttar Pradesh. *International Journal of Remote Sensing*, *22*, 565–593.

Signorini, A., Segre, A. M., & Polgreen, P. M. (2011). The use of Twitter to track levels of disease activity and public concern in the U.S. during the influenza A H1N1 pandemic. *PLoS One*, *6*(5), e19467.

Small, C. (2006). Comparative analysis of urban reflectance and surface temperature. *Remote Sensing of Environment*, *104*, 168–189.

Stefanov, W. L., Ramsey, M. S., & Christensen, P. R. (2001). Monitoring urban land cover change: An expert system approach to land cover classification of semiarid to arid urban centers. *Remote Sensing of Environment*, *77*, 173–185.

Storey, J., Scaramuzza, P., & Schmidt, G. (2005). Landsat 7 scan line corrector-off gap filled product development. *Pecora 16 conference proceedings, 23–27 October 2005, Sioux Falls, South Dakota.*

Tan, M., Li, X., Xie, H., & Lu, C. (2005). Urban land expansion and arable land loss in China — A case study of Beijing–Tianjin–Hebei region. *Land Use Policy*, *22*(3), 187–196.

Tan, B., Morisette, J., & Wolfe, R. (2011). An enhanced TIMESAT algorithm for estimating vegetation phenology metrics from MODIS data. *IEEE Journal of Selected Topics in Applied Earth Observations and Remote Sensing*, *4*(2), 361–371.

Tan, B., Morisette, J. T., Wolfe, R. E., Feng, G., Ederer, G. A., Nightingale, J., et al. (2011). An enhanced TIMESAT algorithm for estimating vegetation phenology metrics from MODIS data. *IEEE Journal of Selected Topics in Applied Earth Observations*, *4*, 361–371.

Please cite this article as: Mertes, C.M., et al., Detecting change in urban areas at continental scales with MODIS data, *Remote Sensing of Environment* (2014), http://dx.doi.org/10.1016/j.rse.2014.09.023

Tatem, A. J., Noor, A. M., von Hagen, C., Di Gregorio, A., & Hay, S. I. (2007). High resolution settlement and population maps for low income nations: combining land cover and national census in East Africa. *PLoS One*, *2*, e1298.

Taubenböck, H., Esch, T., Felbier, A., Wiesner, M., Roth, A., & Dech, S. (2012). Monitoring urbanization in mega cities from space. *Remote Sensing of Environment*, *117*, 162–176.

Verbesselt, J., Hyndman, R., Newnham, G., & Culvenor, D. (2010). Detecting trend and seasonal changes in satellite image time series. *Remote Sensing of Environment*, *114*(1), 106–115.

Wang, L., Li, C., Ying, Q., Cheng, X., Wang, X., Li, X., et al. (2012). China's urban expansion from 1990 to 2010 determined with satellite remote sensing. *Chinese Science Bulletin*, *57*, 2802–2812.

Weng, Q. (2001). A remote sensing-GIS evaluation of urban expansion and its impact on surface temperature in the Zhujiang Delta China. *International Journal of Remote Sensing*, *22*, 1999–2014.

Wilhelmi, O., de Sherbinin, A., & Hayden, M. (2013). Exposure to heat stress in urban environments. In B. King, & K. A. Crews (Eds.), *Ecologies and Politics of Health Book Series*, *41*. (pp. 219–238). Routledge Studies in Human Geography.

World Bank (2014). Mapping a Decade of Urban Change: East Asia, 2000-2010. Washington DC: World Bank Publications (in press).

Wulder, M., Masek, J., & Cohen, W. (2012). Opening the archive: How free data has enabled the science and monitoring promise of Landsat. *Remote Sensing of Environment*, *122*, 2–10.

Yates, D., & Paquette, S. (2011). Emergency knowledge management and social media technologies: A case study of the 2010 Haitian earthquake. *International Journal of Information Management*, *31*(1), 6–13.

Zhang, X. Y., Friedl, M. A., Schaaf, C. B., Strahler, A. H., Hodges, J. C. F., Gao, F., et al. (2003). Monitoring vegetation phenology using MODIS. *Remote Sensing of Environment*, *84*(3), 471–475.

Zhang, Q., & Seto, K. C. (2011). Mapping urbanization dynamics at regional and global scales using multi-temporal DMSP/OLS nighttime light data. *Remote Sensing of Environment*, *115*(9), 2320–2329.

Zhao, S., Zhu, C., Zhou, D., Huang, D., & Werner, J. (2013). Organic carbon storage in China's urban areas. *PLoS One*, *8*(8), e71975 (article).

Zhou, L., Dickinson, R. E., Tian, Y., Fang, J., Li, Q., Kaufmann, R., et al. (2004). Evidence for a significant urbanization effect on climate in China. *Proceedings of the National Academy of Sciences of the United States of America*, *101*(26), 9540–9544.

Zhu, Z., Woodcock, C. E., & Olofsson, P. (2012). Continuous monitoring of forest disturbance using all available Landsat imagery. *Remote Sensing of Environment*, *122*, 75–91.

Please cite this article as: Mertes, C.M., et al., Detecting change in urban areas at continental scales with MODIS data, *Remote Sensing of Environment* (2014), http://dx.doi.org/10.1016/j.rse.2014.09.023